The Design of an Autonomous Jumping Robot: Using Inspiration from a Galaxy Far, Far Away...

Team "Ourknocks" - ME 112

Jack Lane, Sonali Singh, Mario Khosla, Reed Kraus

Mechanical Engineering Design Group
416 Escondido Mall
Stanford University
Stanford, CA 94305-2203

1 Executive Summary

A fully realized design for a jumping robot was the task at hand for each cohort of mechanics attempting the final project of Mechanical Systems Design. The robot, intended to start on from the ground, must convert energy from a battery into stored mechanical energy within 5 seconds and then self-actuate to complete a one-meter jump. The jumping robot must come to rest on the hull of a mock spaceship, which had been conveniently covered in velcro fabric. The only human involvement during this event was to be in flipping a switch used to initiate the jump. Initially, the robots' appearance was meant to mimic the Mynock (infamous for their appearance in Star Wars, jumping and clinging to the hull of the asteroid-stranded Millenium Falcon) but subsequently mostly imitated the motion and appearance of the *Rana temporaria*, a common frog.

Though we iterated through many mechanisms during the course of the project, we settled quickly on a two-legged hopper design. We expected symmetry in the body to be of the utmost importance in a purely vertical jumping. Simply put, the 'Knock is comprised of a six-bar linkage, constrained by two sets of gears at the hip and ankle to reduce its range of motion to one degree of freedom.

We sought to design a robot that was both sturdy and lightweight, as the height of a jump is inversely proportional to weight. In other words, making a robot half as heavy is an easy way to double the jump height. Finally, we oscillated between using springs and rubber bands as energy storage devices, but eventually decided that rubber bands were superior for their lightness and greater range of motion. We eventually attached the rubber bands between the middle of the legs, after experimenting with them on the outside of the upper legs. The whole robot was powered using a Pololu 1000:1 Microgear DC motor, and three 3.7 V Lithium Polymer batteries in series. The materials used were a combination of laser-cut acrylic, lego gears attached to spline axles, and tiny 3D-printed spool hubs on the motor shaft.

Overall, our robot was successful, meeting every specification: it completed the loading phase in under 5 seconds with an 7.25 cm crouched height and 29.5 cm crouched width, jumped 1 meter, and successfully attached itself to the bottom of the spaceship. Key issues along the way involved finding the right energy storage system, initiating the jump after the robot was lowered, and stabilizing the robot during the loading and flight phases. Additionally, the design and dimensions of the legs and base went through many iterations, to balance a powerful loading phase with minimal weight.

Even though the robot functioned as intended, there is significant room for improvement in our design. Our robot was 150 grams and functioned with an overall efficiency of 23.2%. There are areas of the robot with poor material utility, in which more than enough material is used to achieve a factor of safety. A redesign of the robot would heavily emphasize scaling down of size, and the use of lighter, less brittle materials.

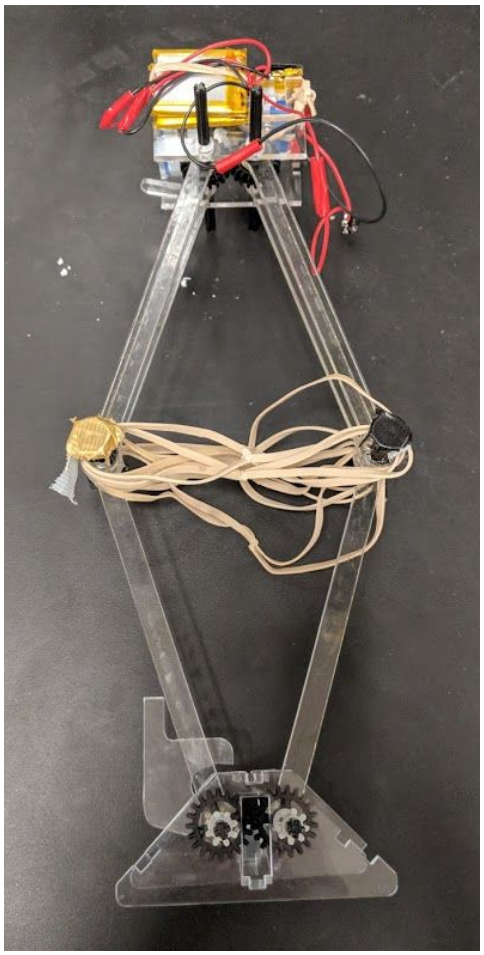

Figure 1: Our jumping robot at rest

Contents

2 Background

2.1 Overview

The goal of this project was to build a robot capable of autonomously jumping at least one meter. The robot was supposed to mimic the Mynock, a fictional creature from the Star Wars universe. Put simply, Mynock movement is almost identical to that of a frog here on Earth. Thus, the project began by figuring out how to best replicate the jumping of a frog.

We began our research by looking at similar bio-inspired robots in a variety of papers. Notably, we investigated insect-inspired jumping (Scarfogliero et al., 2006), single-motor-actuated, two-legged, frog-like jumpers (Zhao et al., 2013), as well as one-legged hoppers analogous to someone jumping on a pogo stick (Plecnik et al. 2017).

The main insight gleaned from perusing the literature on jumping robots is that there are many, equally-effective ways to accomplish the task of jumping. Emphasizing simplicity, we therefore thought about ways to most easily meet the requirements at hand. Given that frogs jump with two legs, we decided to explore a symmetric, four-bar linkage connected at the top and bottom. To prove the simplicity of the concept, we made prototypes using Lego technic cross beams for the body, and placed rubber bands of differing stiffnesses between the legs. We easily achieved the one meter jump height criterion, and thus decided to pursue this design further. Even though other options were considered along the way, solidifying the structure of the robot to be two-legged and symmetric proved to be helpful in focusing our energy into meeting the requirements set forth in the project description.

2.2 Requirements

In order to save Mynocks from extinction, a mock Mynock was to be engineered to prevent live ones from clinging to spaceships. To deliver a robot that met all the requirements, it needed to:

- Start from the ground (hardwood floor), less than 0.3m wide and 0.1m tall crouched;
- Jump within 5 seconds of being activated;
- Be completely autonomous after being activated;
- Stick to the hull of the faux Millenium Falcon, one meter off the ground, which is covered in loop fabric;
- Have all the energy needed to jump be produced by batteries, after activation.

In general, the robot was supposed to appear similar to a Mynock, or a frog (*Rana temporaria*). However, this requirement was easily met by replicating the movement of frogs with a two-legged structure.

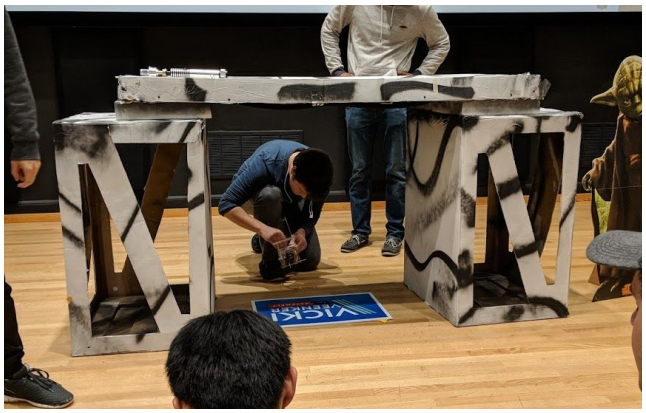

Figure 2: Robo-Mynock testing with the procured hull of the Millenium Falcon

3 Design

We approached this problem with the goal of creating a consistently performing mynock with a reliable and repeatable actuation mechanism whilst overestimating our constraints. As such, we allowed simplicity and straightforwardness to inform our design process, whilst drawing the majority of our inspiration from biomimicry. We have sectioned our paper to reflect our thought process, starting with biomimetic inspiration, continuing onto the linkage design, energy storage considerations and our drivetrain, our overall assembly, and finally, our elegant mechanically-triggered release mechanism.

3.1 Biomimetic Inspiration

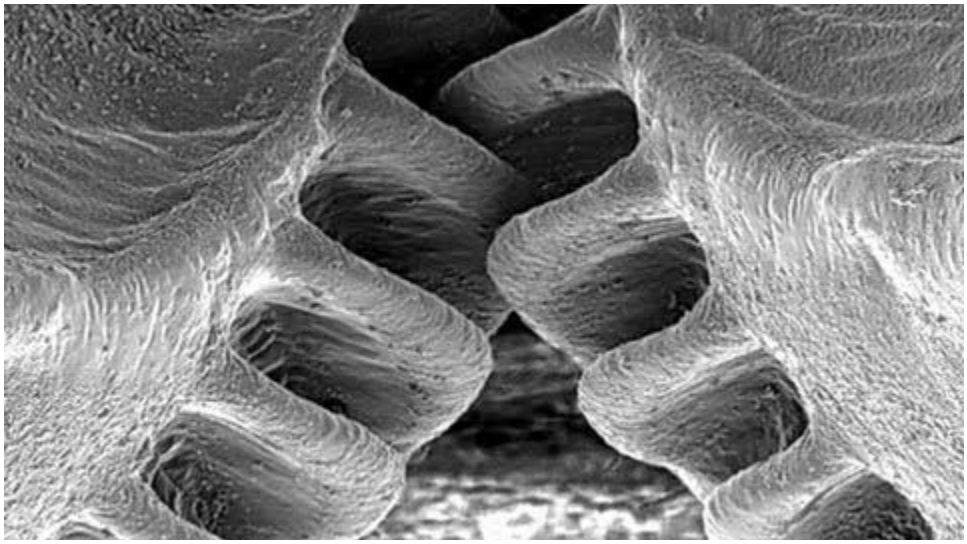

Figure 3.1: The incredible natural gears of the Issus coleoptratus, and insect also commonly known as the plant-hopper, from whom we derived inspiration for the gear pairing features in Ourknock (Cambridge University. "Mechanical gears in jumping insects.").

To simplify this design challenge, we drew inspiration from existing jumping creatures in nature particularly the jumping motion of frogs, such as the *Rana temporaria*, and the physical structure of *Issus coleoptratus*, a plant-hopping insect (Burrows & Sutton, 2013), the natural gears of which we mimicked in our design (Figure 3.1 above). A key difference between the jumping motion of the mynock and the living *Issus* and *Rana temporaria* is the jumping arc which, for the Mynock, is nearly vertical. As such, noting the jumping characteristics in a slow-motion video provided by National Geographic, we noted the positioning of the foot of a typical jumping frog and concluded in a design review that a purely vertical motion necessitates a center of gravity

vertically over the foot of the jumping robot. We chose to mirror image our linkage design to help us achieve this center of gravity, as the *Rana temporaria*, *Issus coleoptratus*, and the Mynock similarly have symmetric legs. Lastly, we chose to model the creature as settles into its takeoff position, presumably falling or returning from a previous jump, compressing and then actuating in one relatively continuous movement which we discuss in our analysis section as two stages - loading and jumping.

3.2 Linkages

We began our process by thinking about linkage combinations that could translate motion in along one axis into stored energy along another axis, shown in Figure A5.1 in Appendix 5. We approached this design problem with Grashof's formula defining degrees of freedom as our predominant focus, defined below:

$$F = 2(N-1) - 2f_1 - f_2 \quad (1)$$

In which F is the degrees of freedom of the linkage system, N the number of links, f_1 the number of type one (pin) joints and f_2 the number of type two (slots, gears) joints. Our first prototype, Figure A5.1, toppled and often did not actuate and further initial prototypes, Figure A5.4, and models experienced a buckling failure at the feet. We drew inspiration from *Issus coleoptratus* to reduce our degrees of freedom from three to one by adding two pairs of gears, one at the hip and one at the ankle of Ourknock.

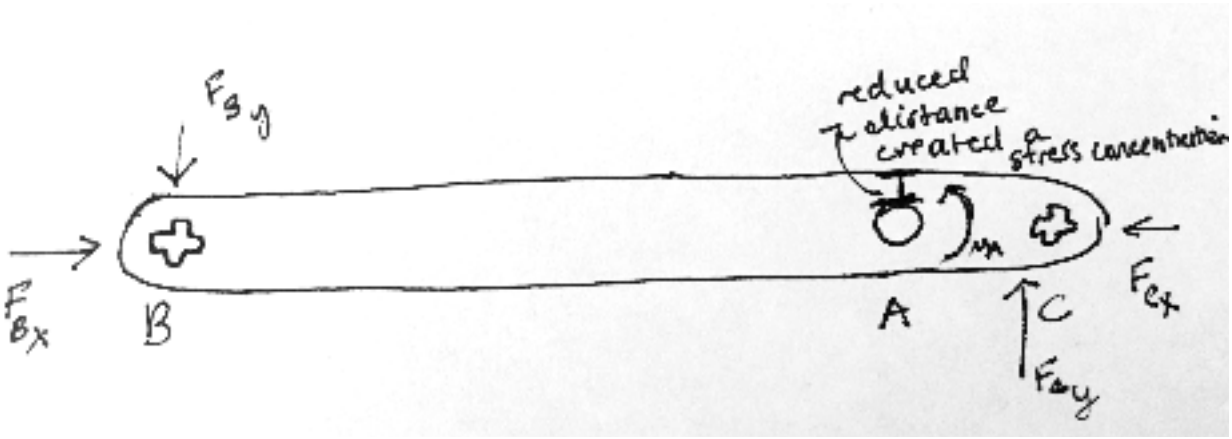

Figure 3.2.1: A free-body diagram of a previous linkage that snapped at point A. We removed the lever arm C to reduce the moment applied at A.

We designed each of our linkages with loading and stress in mind, increasing the moment of inertia around through-holes and using filleting to avoid stress concentrations around our axles, as the inelastic behavior of acrylic rendered our linkages prone to breakage, further examples of

which are noted in Figure A5.5 in Appendix 5. A free-body diagram of one of the links is shown above in figure 3.2.1.

Figure 3.2.2: Calf link, no angle in the axle profile.

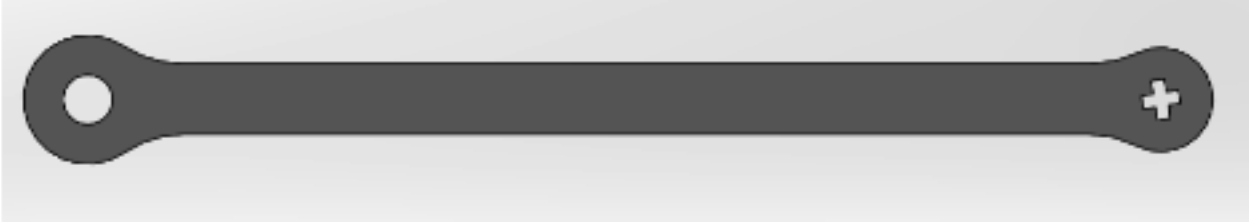

Figure 3.2.3: Thigh link, axle profile angled by 9 degrees (half of a gear tooth) to ensure vertical alignment during compression and takeoff.

We included the lego axle profile in our linkage to restrict the rotation of the linkage lego-gear constraint combination, effectively pinning the lego gear to the link (figures 3.2.2 and 3.2.3 above). We drew further inspiration from the behavior of the *Rana temporaria* in our linkage and foot design, increasing the length of the calf and thigh linkages to 13.75 cm to increase the time of leg extension and thereby foot contact time with the floor for a greater overall impulse delivered to Ournock.

3.3 Energy Storage

We chose to use rubber bands as the preliminary energy storage mechanism of our jumper. Rubber bands showed a significant advantage over metal springs in a number of ways. For one, rubber bands are able to stretch to a much greater multiple of their natural length than a spring of equivalent stiffness. This allowed us to put rubber bands across the knees of Ourknock, which start about ten centimeters apart but extend to just under thirty centimeters at peak loading as the jumper compresses.

Additionally, rubber bands are able to store much more energy per unit of mass than springs (Steve Collins, Mechanical Systems Design Lecture, 3/9/18). This meant that we would be able to get the required force to jump one meter while maintaining a lower total jumper mass. If we had used springs, more springs would have been required to achieve the same liftoff force as our

rubber bands. The extra weight of these additional springs become a utility problem, as more weight requires more energy stored in springs and increases the torque needed from our motor to compress them.

Rubber bands were interchangeable from a large and cheap supply purchased online, while springs would have needed more careful specification and replacement. Finally, rubber bands are less fragile, more easily replaceable, and much cheaper than springs. This allowed us to cut costs and conduct testing without worrying about spring replacement.

3.4 Motor, Batteries, and Transmission

The drivetrain of our jumper is comprised of the batteries, a Pololu electric motor with integrated transmission, and a 3D-printed spool around which string is wrapped to compress the jumper. The motor used in our jumper, shown in figure 3.4, is a Pololu 1000:1 micro metal DC gearmotor, delivering a stall torque of 125 oz-in, or about 0.88 Nm. At no load, the angular velocity is 32 rotations per minute at 6V. It has a cross section of 10 × 12 mm, and the D-shaped gearbox output shaft is 9 mm long and 3 mm in diameter. Despite being rated to operate at 6 V, we applied 11.63 V to the motor during testing. This significantly higher operating voltage is acceptable, since we limited the overdrive to the motor to 5-10s intervals. Overheating was therefore one of our biggest concerns with motor failure, and extra precaution was taken to turn the system off immediately after a test run.

Figure 3.4: The micro metal gearmotor used in our robot, coupled to a 1000:1 speed reduction. Image from https://www.pololu.com/product/1595, accessed March 19, 2018.

The batteries chosen were three Lithium-Polymer cells, each with an operating 3.88V and 500mAh. These were combined in series to achieve the final 11.63V number needed to move the motor fast enough to wind down the full jumper compression in five seconds. The batteries were

chosen for their energy density, being relatively lightweight, and for their internal resistance values, which allowed the motor to draw more current for higher torque (torque is linearly proportional to current).

Spool sizing was especially important for our project, as we wanted to make sure we would be able to compress the jumper in the required five seconds, but also needed to make enough torque to be able to compress the necessary amount of rubber bands to jump to one meter. A fuller digression and analysis are included in section 4.1.4. We determined the required spool size by utilizing the smallest size that would be able to compress the full 200mm compression of the jumper legs within the five second winding period. By significantly increasing our voltage and current, we were able to ensure that we could both descend quickly enough and also produce enough torque to stretch all of the rubber bands required to jump one meter.

3.5 Assembly

The major parts of the jumper are made from laser-cut acrylic. This material was chosen for its relatively light weight, ease of cutting, and variability of thicknesses available. We were able to optimize parts like the leg links and the upper housing faceplates by cutting them out of thicker and thinner sheets of acrylic, respectively. Acrylic also provided a stiffness advantage over duron laser-cut parts.

Our jumper is held together with lego axles and spline holders, press-fit acrylic links, and nylon shoulder screws. The legos hold together the feet and the upper housings, which encase the lego gears mounted on lego spline axles. The feet and upper housings derive additional rigidity from laser cut acrylic crossbars, which were iterated and sized to fit very tightly into laser cut holes on the foot and upper housing faceplates. The knee joint of our jumper consists of a nylon shoulder screw on each side, which holds together two upper links and one lower link. The hole size on the links was set specifically to allow for very little play on the shoulder screw, while still having enough gap to rotate freely and not encumber the jumping motion.

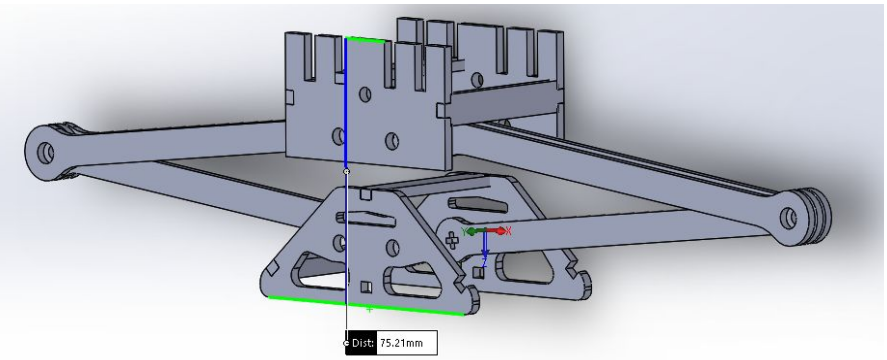

Figure 3.5.1: CAD render of jumper in the approximate compressed height (7.52 cm), after exactly 5 seconds of loading

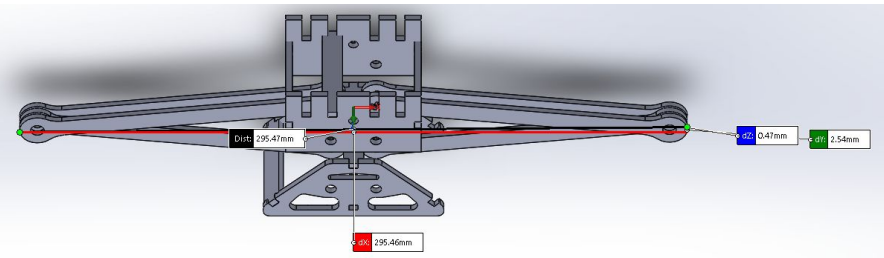

Figure 3.5.2: CAD render of jumper's largest compression width (29.5cm), just under the 30 cm width restriction

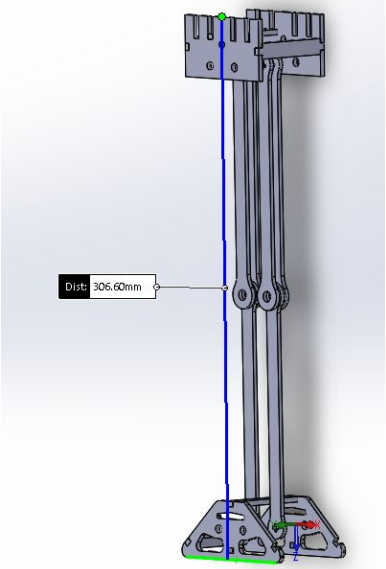

Figure 3.5.3: CAD render of robot in the fully extended position, a maximum height of 30.6cm

Our jumper extends to about 29.5 cm, just under the width limit of 30 cm, as shown in Figures 3.5.1-3. Additionally, our compressed height is approximately 7.5 cm, which is comfortably under the 10 cm height restriction (figure 3.5.2). Our jumper reaches a full extension height of about 30.6 cm (figure 3.5.3). As during its performance our jumper was able to compress and actuate in exactly 5 seconds, we note that our robot met all of the specifications outlined in the project document.

3.6 Release Mechanism

We chose a string and spool system to convert the torque into useful compressive force for our linkages, rather than relying on the torque supplied from our motor and a gear train to power a linkage system.

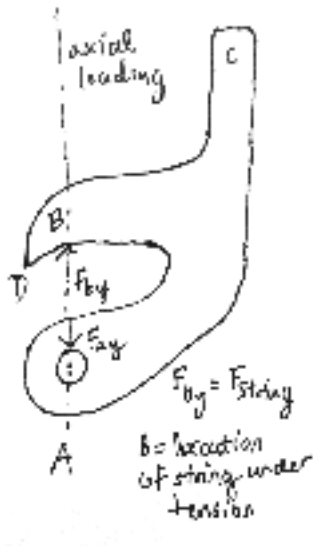

Figure 3.6.1: A free-body diagram of our release mechanism, modeled from the triggering mechanism of a rubber band gun. The force from the string on the hook may have non-zero x component ($F_{s,x}$), as well as a frictional component that contributed to losses.

We chose an intermediary between the ratchet-release and bistable methods, drawn in figure A5.3 of the appendix, to actuate Ourknock's jump. Our release mechanism is restricted by a length of string (dental floss) wound around a spool connected at the shaft of our motor. The mechanism is stable during loading, acting as a two-force member with the only forces applied along the y axis.

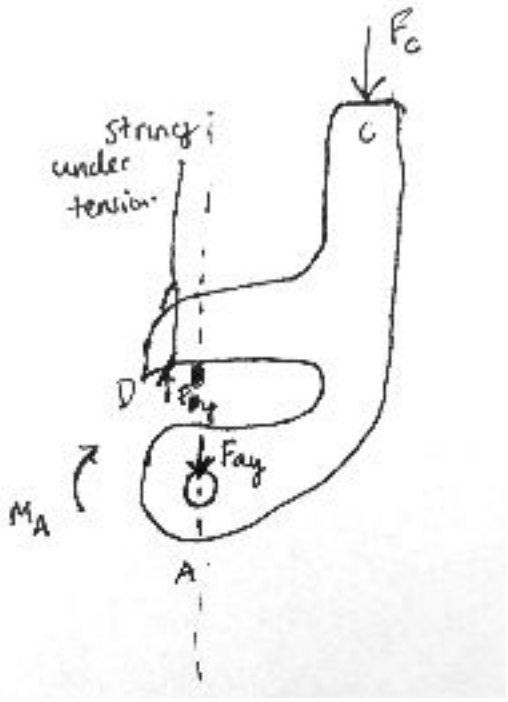

Figure 3.6.2: The trigger mechanism as a load from a crossbeam is applied and a moment created around the fixed point A. The mechanism is no longer in equilibrium and rotates until the string force is no longer applied (the string falls off at point D).

When Ourknock compresses to its loaded height, a crossbeam applies a downward force to the trigger mechanism at C, creating a moment around the axle shaft at A. The mechanism, no longer in equilibrium, rotates about the fixed point A and the loop of string, still in tension, slips off of the mechanism at point D, allowing Ourknock to actuate its jump. Figure 3.6.2, shown above, is a free-body diagram illustrating this concept.

4 Performance Analysis

Description of our approach to the performance analysis

4.1. Loading

4.1.1: Energy Storage

As mentioned above, the loading phase of the robot took approximately 5 seconds. To store energy, we primarily used compound rubber bands: two bands of equal natural length and elasticity, tied together at the middle. In the final iteration of the robot, there were 6 sets of these rubber bands, three on each side, as shown in figure 4.1.1 below.

Figure 4.1.1: Rubber bands knotted together to extend their operating length and vary the phase of their engagements stored energy during the loading phase of the jump.

During the final days of designing the jumper, a lot of time was spent fine-tuning the stiffness of the effective combination of bands in between the legs. In the end, the elastic constant in equation 1, k, turned out to be 98.5 N/m:

$$F = k*x \tag{2}$$

where F is the tensile force in the “effective” rubber band (a combination of all 6 sets, lumped together as one band), and x is the difference in stretched length and unstretched, or natural, length. Lumping the 6 sets of rubber bands together is problematic because not only is each band a non-linear spring, we also used pairs of differing band type. However, the elastic constant above measures the stiffness of the lumped bands once they all begin to stretch. In other words, until the third set on each side engages, their is a slightly lower effective stiffness of the bands between the legs. Given the exceedingly short duration that not all bands are stretched while the robot is lowering, it can be assumed that the elastic constant of 98.5 N/m is constant throughout

the 5 second loading phase. Additionally, the rubber bands are not pre-loaded, meaning they begin in a "slack" position until the motor is turned on.

A linear model of the rubber bands results in the following curve shown in figure 4.1.2:

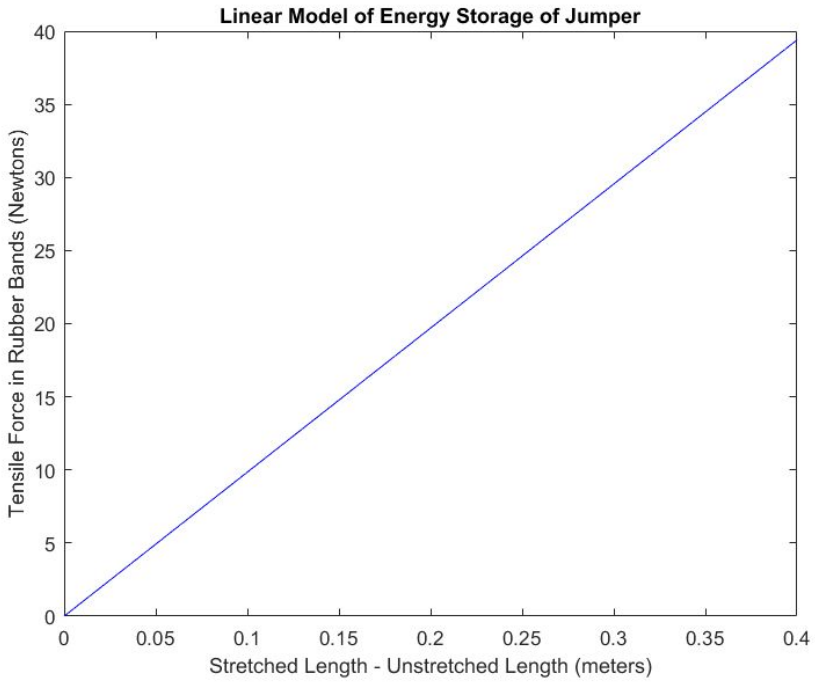

Figure 4.1.2: A linear model of the lumped rubber bands, with a slope of 98.5 N/m (k in Equation 1). Even though rubber bands individually behave as non-linear springs, and we used different types of bands, we assume that all 6 sets of bands attached between the middle of the legs act effectively as one linear spring.

The bands stretch from 16.5 cm, their natural length, x_{min}, to about 28 cm, fully stretched, x_{max}. The total amount of energy stored in the spring can be computed from the area under the curve between the start and end of the loading phase, via equation 2:

$$E_{rubber\ bands} = \frac{1}{2} * k * (x_{max}^2 - x_{min}^2) \quad (3)$$

where E_{bands} is energy stored in the bands, k is the elastic constant, x_{min} is the unstretched length of the bands, and x_{max} is the stretched length of the bands at the end of the 5 second lowering phase. Therefore, we store approximately 2.52 Joules by stretching the rubber bands between the legs in the loading phase.

4.1.2: Energy Input from the Motor

Now that we have an approximate quantity of how much energy was stored in the rubber bands during the loading phase, we can compare that to the energy input from the motor. The lowering mechanism was a piece of string attached to a spool on the motor shaft, connected to the robot's base. A static lowering test showed that it took about 3 kg of mass to fully lower the robot. This is the amount of mass it takes to lower the robot at its most force-intensive point. Using equation 3, we can calculate the approximate, constant force in the string during lowering:

$$F = m*g \tag{4}$$

Where m is the mass required to lower the robot, and g is the acceleration due to gravity (9.81 m/s^2). Therefore, we calculate that the force in the string to lower the robot is 29.43 Newtons. Since a spool of 6 millimeters in radius was coupled to the motor shaft on test day, the maximum torque needed to fully lower the robot is calculated using equation 4:

$$T_{shaft} = F_{string} * r_{spool} \tag{5}$$

where T_{shaft} is the motor torque, F_{string} is the maximum string force, and r_{spool} is the radius of the spool. Therefore, the torque required to fully lower the robot is 0.130 Nm. For simplicity, it can be assumed that this upper bound of force, F_{string} is constant in the lowering phase, which will result in a conservatively high estimate for energy input by the motor. We now need to know the starting height and ending height of the jumper. The vertical change in distance is measured to be about 23.14 centimeters, which is illustrated in figure 3.5, above. An estimate of the energy input by the motor to lower the robot is found using equation 5:

$$E_{motor} = F_{string} * dy \tag{6}$$

where E_{motor} is the energy input by the motor, F_{string} is the "constant" force in the string, and dy is the change in height during loading. Thus, a conservative estimate for energy input by the motor is about 6.81 Joules. The energy stored in the rubber bands divided by the energy input by the motor yields a rough efficiency of 37% during the loading phase.

4.1.3: Losses

The efficiency calculated of 37% is a rough estimate. Friction during lowering in the pin joints connecting the legs is one potential source of energy loss. Additionally, the force of the string might not have been directed purely upward, meaning the motor would have to work harder than necessary. These are just a couple of potential sources of error that contributed to hefty losses in transferring work from the motor's shaft to stretch the rubber bands.

4.1.4: Spool Sizing, Speed and Strength Tradeoffs

We produced a series of graphs that helped inform our decision on the proper spool diameter to use in conjunction with our motor. Knowing the motor's specification of 32 rpm and 0.88 NM of torque at 6v and 120 mAh, we were able to put together a plot showing us how much string we could wind down in the target time of five seconds, as well as how much pull force we would be able to exert to compress the jumper. From non-motor driven testing, we knew the maximum compression force needed to reach one meter jumping would be around 30 N. Based on our jumper's dimensions, we would need to pull about 200 mm of string to fully compress. The equations used to calculate were as follows:

$$l_{string} = \omega * r_{spool} * 5s \tag{7}$$

$$F_{string} = T_{motor} / r_{spool} \tag{8}$$

As can be seen from the graph below, there was no way to achieve the necessary motor torque to exert enough pulling force to compress the jumper, while also pulling enough string in five seconds to go through the entire jumping motion. Our options were limited to using a smaller spool and taking longer to wind down, or upping motor voltage and current by using more battery power.

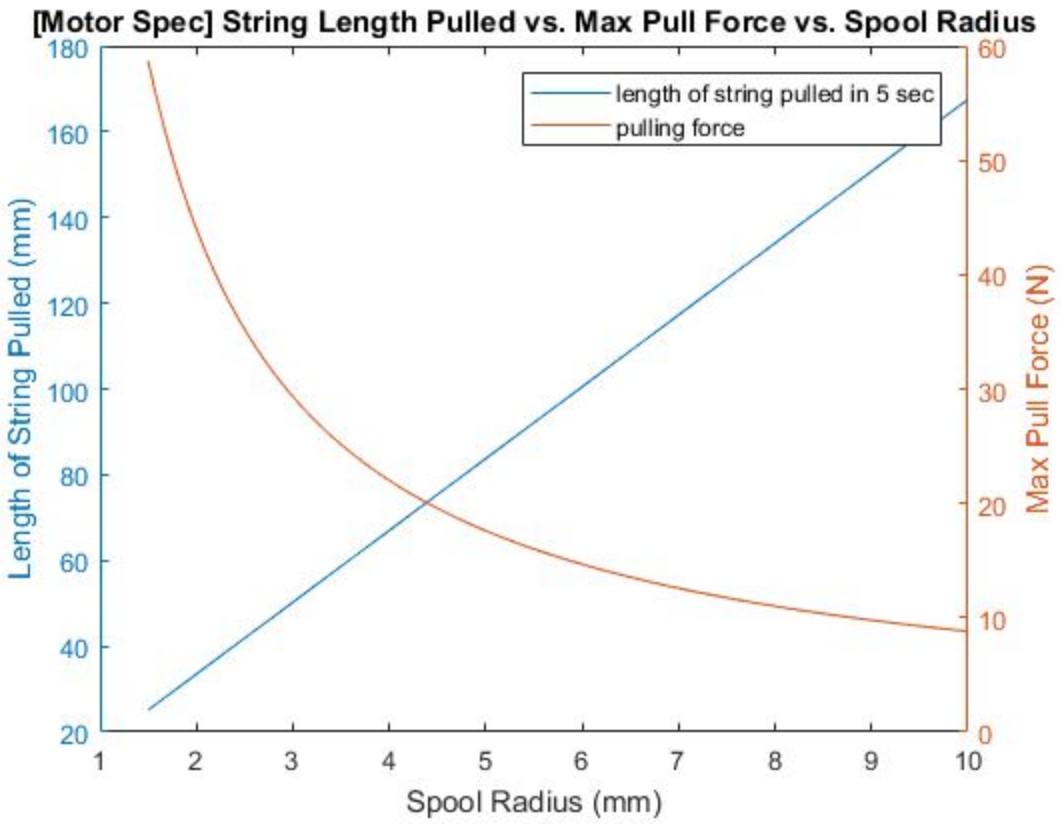

Figure 4.1.3: Motor Rated Voltage and Current Plot

The second graph, below, shows new estimations using three batteries in series. We were able to achieve a voltage of 11.63V to the motor, nearly doubling our motor speed as motor speed scales with voltage. This in turn allowed nearly double the string to be wound up in five seconds. Assuming the current drawn it is near the 500 mA, we can determine an upper bound for the maximum output force from the motor for a given spool size, as torque scales with current through the motor. We chose the smallest spool that would wind enough string to compress the jumper, which can be determined to be about 12 mm in diameter.

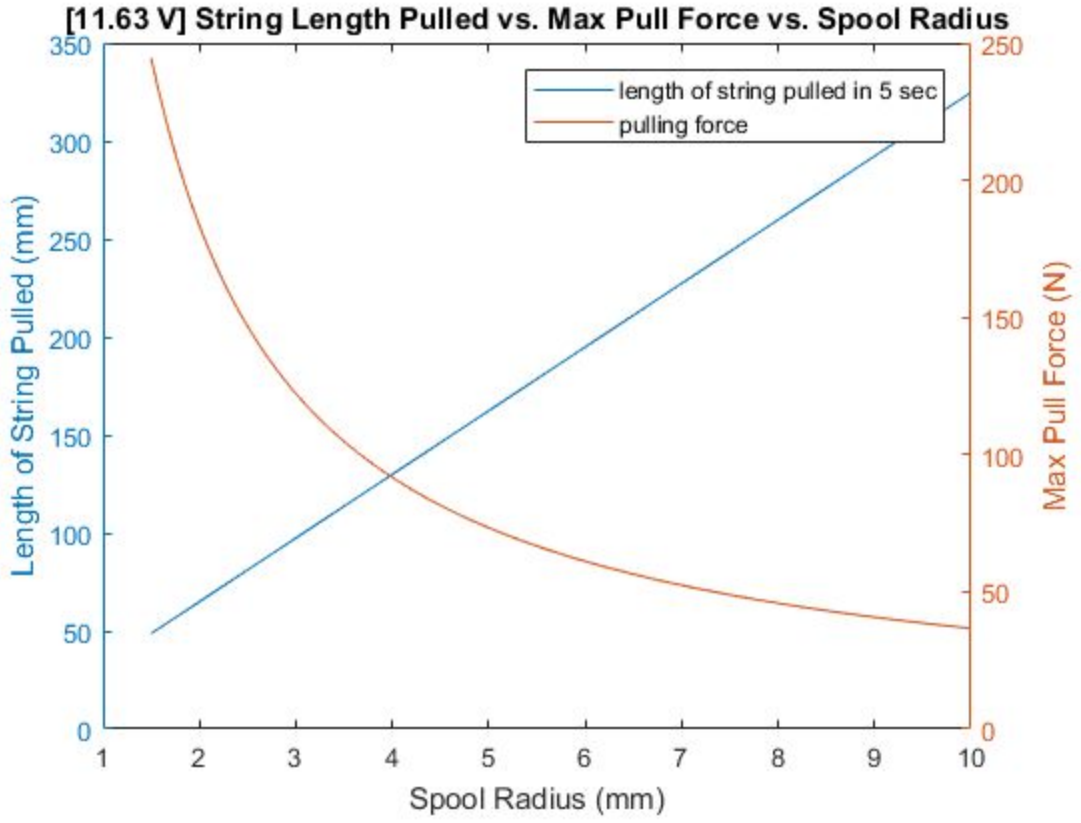

Figure 4.1.4: Higher Voltage and Current Plot

Figure 4.1.4 demonstrates that this diameter allows us put us comfortably more than the necessary compression force to load our robot; however, in actuality, the motor torque is somewhat lower due to induced current losses from the rotating motor windings.

4.2 Jumping

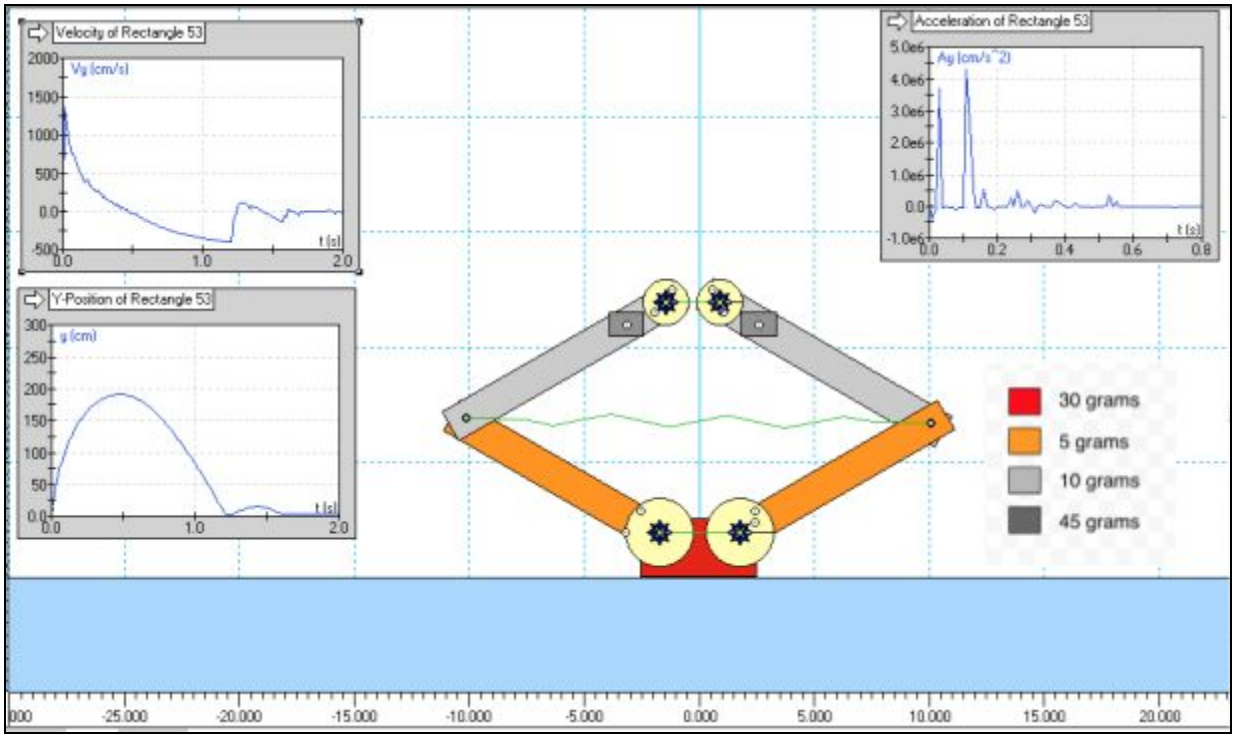

Figure 4.2: A working model simulation of our mynock, which experienced a peak y-velocity of 15 m/s and traveled approximately 1.9 m.

We simulated our mynock in working model, with an overall weight of 150 grams, distributed as shown in Figure 4.2. Our mynock simulation included an air resistance k of approximately $1.29*10^{-3}$ kg/m, characterised by the equation:

$$F = \frac{\rho * C_d * A}{2} * v^2 = k * v^2 \quad (9)$$

Using the ρ value for air, 1.224 kg/m^3, a cross sectional area of 0.0021 m^2 and a conservative drag coefficient of 1. Based upon this model, our robot should be able to jump approximately 1.71 meters. Analyzing this model further, and noting the following equations for potential (PE) and kinetic (KE) energy:

$$PE = m * g * h \quad (10)$$

$$KE = \frac{1}{2} * m * v^2 \quad (11)$$

Where m is the mass of the simulated mynock in kg, v is the maximum y-velocity of our simulated mynock, approximately 13.25 m/s, g is downward acceleration due to gravity, 9.81 m/s^2, we see that the maximum potential energy of the simulation is 2.52 Joules, and the maximum instantaneous kinetic energy, at takeoff, is approximately 13.17 Joules. Noting our value for v_{max}, we note that the maximum force due to air resistance in our simulation was approximately 0.226 N, occurring at takeoff and corresponding to approximately 23.1 additional grams of weight at that point.

On test day, Ourknock's jump was interrupted by the hull of the Millenium Falcon. Later on test day, modifications were made to the robot to achieve the highest possible jump, and the state of the robot was later reset to its Falcon-touching state. Our uninterrupted experimental mynock jumped approximately 1.07 m vertically, corresponding to a potential energy of 1.57 Joules.

The working model simulation of Ourknock is an approximate, as our at v_{max} at takeoff was likely far below the simulation value (likely somewhere between 4.9 m/s and 5.8 m/s, with a lower bound condition of the potential energy needed and an upper bound of the potential energy stored in the rubber bands). As such, using working model to estimate efficiency in this phase is not a robust method of measuring efficiency; that said, our working model estimate shows an actual loss in height of approximately 0.64m, yielding a 37.4% loss in height and an approximate value for efficiency at 62.6%.

A perhaps more robust method of measuring efficiency at this stage is to look at the change in potential energy from elastic to gravitational. To do so, we can directly compare the energy stored in the rubber bands, E_{in} at 2.52 Joules, to the maximum potential energy of our jumper, E_{out} at 1.57 Joules.

$$\eta = \frac{E_{out}}{E_{in}} \tag{12}$$

This model yields an efficiency of 62.3%, a value close enough to the value calculated using working model, giving some amount of credence to the reliability of both models.

Assuming a relatively accurate calculated air resistance simulation, further losses during the jumping phase can be attributed primarily to friction, losses in collisions, and rotational kinetic energy, given by the following equation:

$$KE_{rotational} = \frac{1}{2} * I * \omega^2 \tag{13}$$

Where I is the moment of inertia about a defined axis and ω the angular speed during rotation. Our mynock tilts very slightly during its due to the weight distribution of the motor and batteries on its torso. This shift can be modeled as rotational kinetic energy, using 0.39 rad/s as our

angular speed from observation, and an I_z of $7.42*10^{-7}$ m^4 with the z-axis out of the plane, we can define the rotational kinetic energy as effectively zero. Frictional losses would have occurred in the pin joints, which we attempted to minimize by reducing the surface area of contact, using aluminum axles with a smaller circumference than initial prototypes, shown in figures A5.6 in Appendix 5. Ourknock's legs were a source of loss in collisions, as screen captures of a test run reveal that the knees knock together twice before the mynock reaches the helm of the Millenium Falcon, shown in Figure A6.1 in Appendix 6.

4.3 Overall Efficiency

We have two primary models for calculating the overall efficiency of our robot. The first being calculating the efficiencies at the loading stage and jumping stage using working model and multiplying those efficiencies for an overall value, and the second, looking at loading state with the conversion of elastic potential energy into gravitational potential energy during the jumping stage. The two values are sufficiently close, within a margin of error, to be able to be used interchangeably.

We calculate the overall efficiency using stagewise efficiency value. Coupling the lowering efficiency of 37% with the jumping efficiency of 62.6%, we calculate that the overall robot efficiency is 23.2%. Using Equation 1:

$$\Delta h = \eta / (m * g) \tag{14}$$

where Δh is the change in height of the center of mass of the jumper, η is the overall efficiency, m is the mass of the jumper, and g is the downward acceleration due to gravity, we calculate a change in height for every Joule of energy input into the system. This means that for every Joule of work output by the shaft of the motor, Ourknock experiences a change in gravitational potential energy of 0.23 Joules. In other words, Ourknock jumps approximately 0.158 meters for every Joule input into the system from the motor.

5 Jumper Redesign

Our robot fared well on test day; it successfully wound itself into a crouched position in under 5 seconds, jumped one meter, and attached its torso to the loop-covered hull of the mock Millenium Falcon. However, as much last-minute fine-tuning was necessary to achieve this success, it is evident that the design can be further optimized.

First, our robot was heavier than necessary; the total weight was 150 grams. During testing, we had a couple of failures in the leg links and base of our robot, due to fracturing of the acrylic. Sudden shocks of concentrated force in jumping and landing, coupled with stress concentrations in the design, caused these failures.

To address strength issues, we added additional material where we thought failure was likely, and used fillets to avoid stress concentrations, as depicted in figure 5.1, above. Though this strategy protected the final design from failure during testing, it could be considered an example of overdesigning and therefore adding unnecessary weight to our jumper. Additionally, many parts, such as the base and the motor housing, depicted in Figure 5.1, had low material utility given the relatively small forces acting on these members.

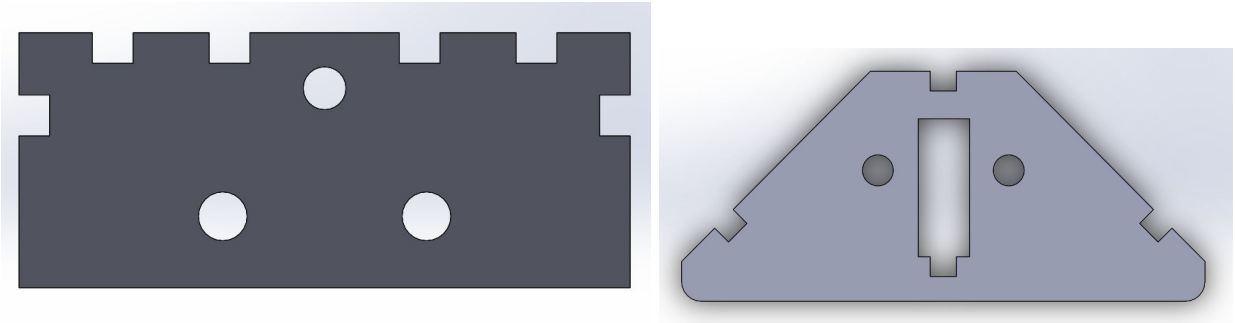

Figure 5.1: Side views of housing for the motor (left), and base of the jumper (right)

In a nutshell, these parts could be redesigned to save on weight by prioritizing material where forces are high, and eliminating material where there are small, or no, forces (e.g. on the bottom left and right corners of the motor housing). Additionally, we could manufacture the jumper's body parts out of a lighter, stronger, materials such as composite wood or reinforced plastics. A reduction in weight would potentially mean fewer rubber bands to jump equally as high, and less required power input by the motor to lower the system, therefore reducing the number of batteries, and overall weight further.

Lastly, a redesign of this robot should prioritize a perfectly vertical jump. Our robot jumped mostly straight in the air, but has a slight deviation from a perfectly vertical path, and has a small amount of rotation in the air. Two factors could be causing this: a ground reaction force accelerating the robot's center of mass that is not directly perfectly upwards, as well as a center of mass that is not aligned with the jump trajectory. The first factor would result in unnecessary horizontal translation, and the latter would cause the robot to rotate in the air. To alleviate such issues, it is prudent to locate the center of mass, find where the ground reaction forces occur on the base of the robot, and ensure that they are aligned vertically.

7 Bibliography

U. Scarfogliero, C. Stefanini, and P. Dario, “A bioinspired concept for high efficiency locomotion in micro robots: The jumping robot grillo,” in Proc. IEEE Int. Conf. Robot. Autom., May 2006, pp. 4037–4042.

Zhao, Jianguo, et al. "MSU jumper: A single-motor-actuated miniature steerable jumping robot." IEEE Transactions on Robotics 29.3 (2013): 602-614.

Plecnik, Mark M., et al. "Design exploration and kinematic tuning of a power modulating jumping monopod." ASME Journal of Mechanisms and Robotics 9.1 (2017).

Burrow, and Sutton. “Interacting Gears Synchronize Propulsive Leg Movements in a Jumping Insect.” Science 341(6151):1254-6 (2013).

National Geographic. “Frog Jumps Caught in Slow Motion | National Geographic.” *Youtube*, 14 May 2010, https://www.youtube.com/watch?v=yKpJElwama8.

Cambridge University. “Mechanical gears in jumping insects.” *Youtube*, 13 Sept. 2013, https://www.youtube.com/watch?v=Q8fyUOxD2EA.

8 Appendix

A1 Terms and Definitions

Symbol	Definition	Units
V	Voltage	Volts
i	Current	Amps
r_{spool}	Radius of the spool on the motor shaft	meters
g	Acceleration due to gravity	meters/s^2
l_{string}	Length of the string wound around the motor shaft during lowering	meters
F	Force	Newtons
E	Energy	Joules
k	Spring constant	Newton/meter
x	Displacement of spring	meters
dy	Change in height of jumper	meters
ρ	Density of air	kg/$meter^3$
C_d	Coefficient of drag	unitless
A	Frontal area	$meter^2$
v	velocity	meter/sec
KE	Kinetic energy	Joules
PE	Potential energy	Joules
ω	Angular speed	radians/second
I	Moment of inertia	kg * $meter^2$
η	Efficiency	unitless
τ	Torque	Newton*meter
P	Power	Watts

A2 Equations

$$F = 2(N-1) - 2f_1 - f_2 \quad (1)$$

$$F = k*x \quad (2)$$

$$E_{rubber\ bands} = \tfrac{1}{2} * k * (x_{max}^{\ 2} - x_{min}^{\ 2}) \quad (3)$$

$$F = m*g \quad (4)$$

$$T_{shaft} = F_{string} * r_{spool} \quad (5)$$

$$E_{motor} = F_{string} * dy \quad (6)$$

$$l_{string} = \omega * r_{spool} * 5s \quad (7)$$

$$F_{string} = T_{motor} / r_{spool} \quad (8)$$

$$F = \frac{\rho * C_d * A}{2} * v^2 = k * v^2 \quad (9)$$

$$PE = m * g * h \quad (10)$$

$$KE = \tfrac{1}{2} * m * v^2 \quad (11)$$

$$\eta = \frac{E_{out}}{E_{in}} \quad (12)$$

$$KE_{rotational} = \tfrac{1}{2} * I * \omega^2 \quad (13)$$

$$\Delta h = \eta / (m * g) \quad (14)$$

A3 Matlab Code

Spool Size Graphs Code:

```
clc;
clear all;
close all;

t_motor = 0.88*500/125; %nm
r_spool = linspace(1.5, 10, 20)
w_motor = 3.351*11.63/6; %rad/s
% string disp. = w*time*r
% time = string disp. / w*r
%sptring displacement = 0.21m on final jumper
winding_time = 5; %seconds

string_displacement = w_motor.*winding_time.*r_spool
pulling_force = t_motor./(r_spool./100)

yyaxis left
plot(r_spool, string_displacement);
ylabel('Length of String Pulled (mm)');
hold on
yyaxis right
plot(r_spool, pulling_force);
ylabel('Max Pull Force (N)');
xlabel('Spool Radius (mm)')
legend('length of string pulled in 5 sec', 'pulling force');
title('[11.63 V] String Length Pulled vs. Max Pull Force vs. Spool Radius')
```

A4 Matlab Data

Spool Size Graph Data:

Spool Radius (mm)	String Pulled in 5 Sec. (mm)	Max Pull Force (N)
1.5	48.71516	234.6667
1.947368	63.24425	180.7568
2.394737	77.77333	146.989
2.842105	92.30241	123.8519
3.289474	106.8315	107.008
3.736842	121.3606	94.19718
4.184211	135.8897	84.12579
4.631579	150.4187	76
5.078947	164.9478	69.3057
5.526316	179.4769	63.69524
5.973684	194.006	58.92511
6.421053	208.5351	54.81967
6.868421	223.0642	51.24904
7.315789	237.5932	48.11511
7.763158	252.1223	45.34237
8.210526	266.6514	42.87179
8.657895	281.1805	40.65653
9.105263	295.7096	38.65896
9.552632	310.2387	36.84848
10	324.7678	35.2

A5 Prototyping and Iterations

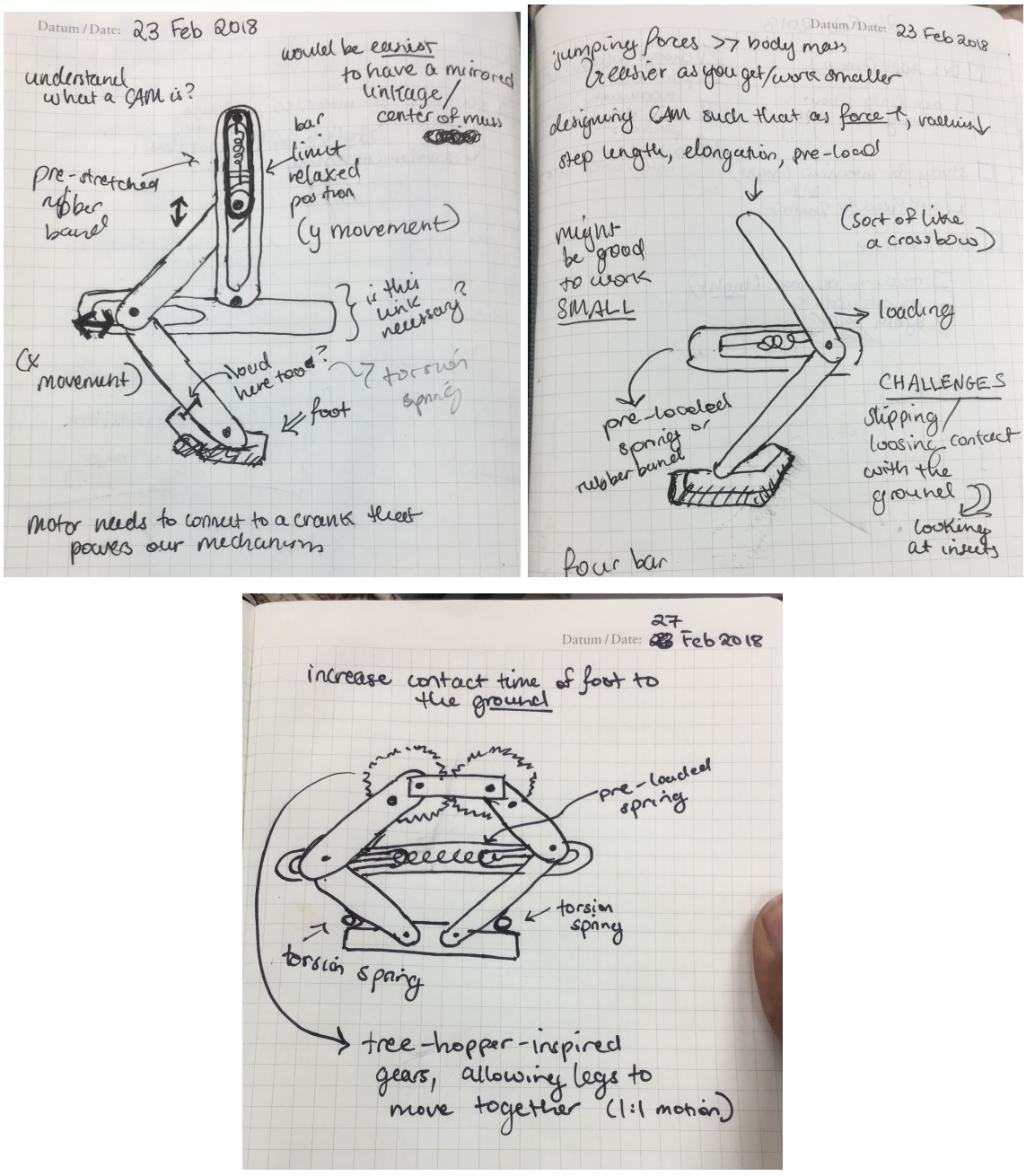

Figures A5.1: Drawings of ideas for linkages that would achieve movement in the y direction from loading and energy storage in the x direction.

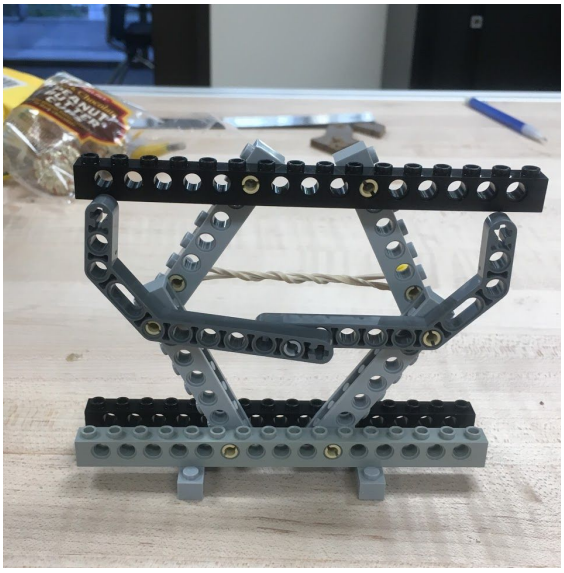

Figure A5.2: A Day Zero prototype of a jumping Mynock. The prototype has 3 degrees of freedom and experienced buckling failures at the torso and the feet. The prototype is also an example of a bistable trigger mechanism.

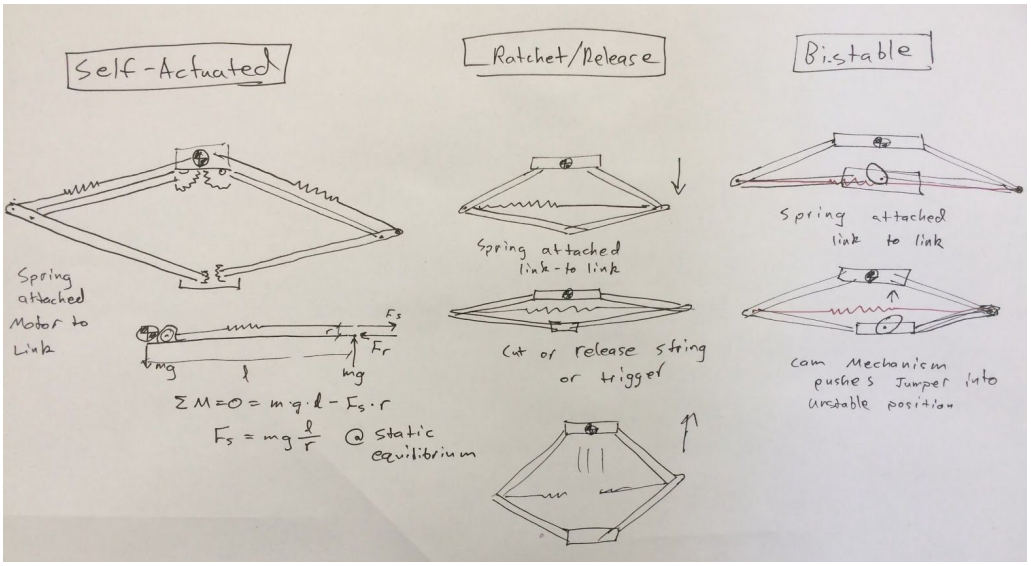

Figure A5.3: concepts for jump initiation - a self-actuated model, a ratchet and release, and a bistable release mechanism

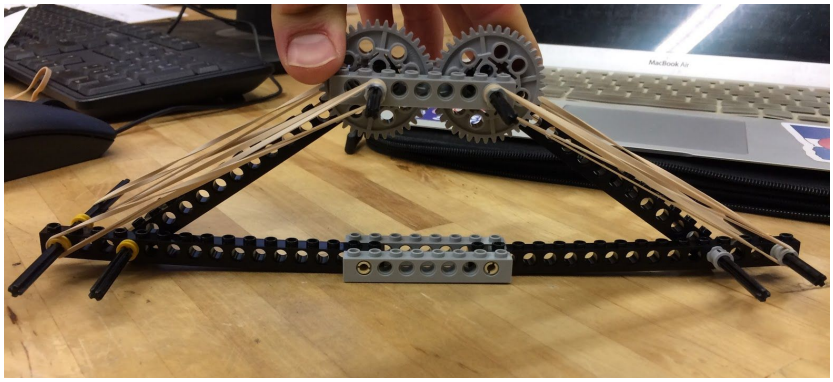

Figure A5.4: lego prototype of a self-actuating jumper with a lever arm and rubber bands emulating thigh muscles, which we initialized via compression

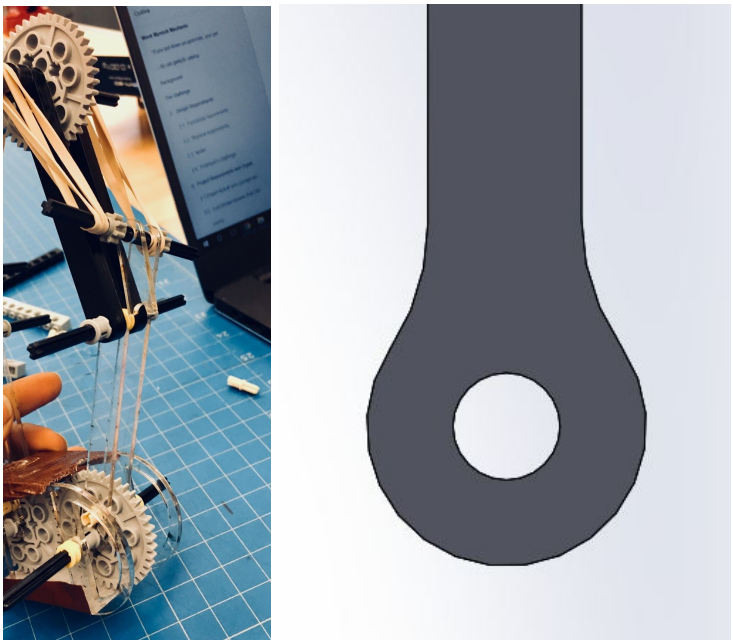

Figure A5.5: Left: failure mode at through-hole for pin connection due to a stress concentration at the diameter of the axle. Right: design solution added additional material around holes and filleting to reduce the stress concentration.

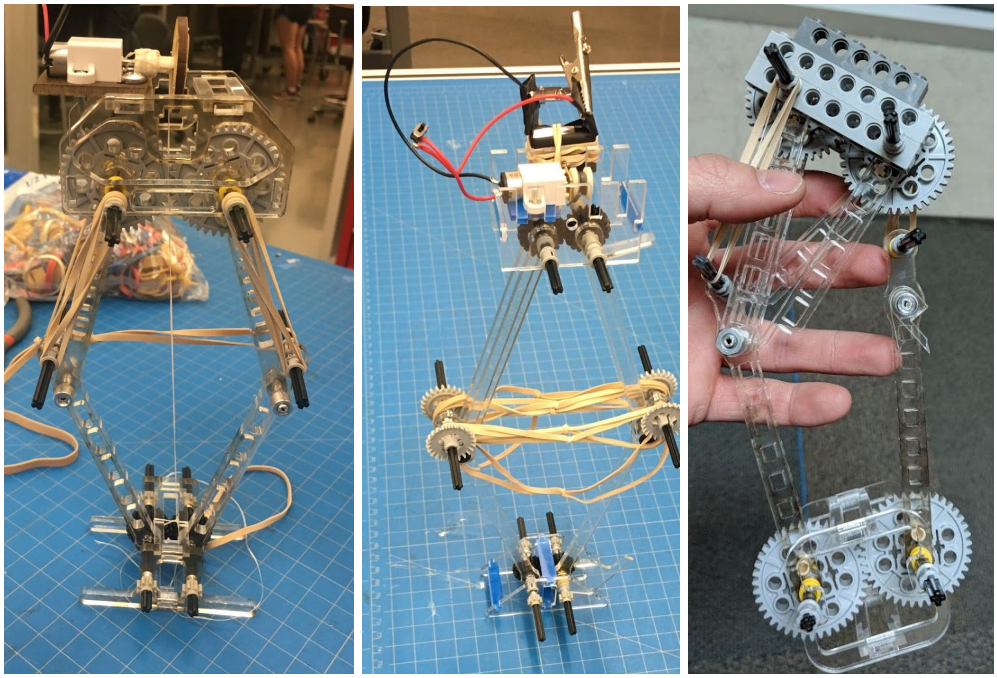

Figures A5.6: Left: rubber bands attached in the middle on pin joints and on the outer edges of the bottom legs, analogous to the self-actuating case. Middle: rubber bands in the middle. solely attached to axles on the outer edges of the bottom legs. Right: Bands on the outside, solely attached to axles on the outer edges of the bottom legs. Failure mechanism was stress concentration in the 'lightening' holes

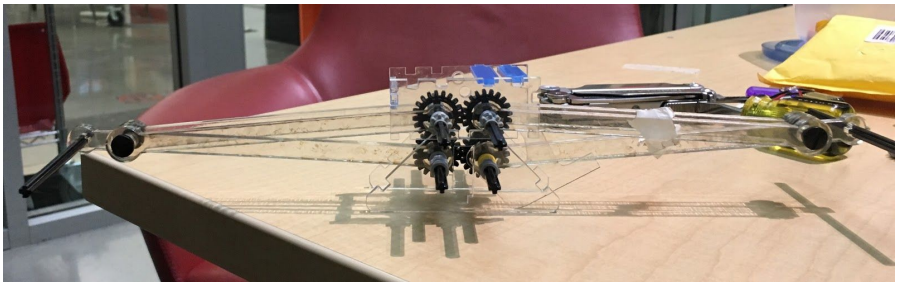

Figure A5.7 Robot design in the crouched position. Additional changes were made to decrease the crouched width and reduce the amount of friction in the pin joints.

A6 Final Design and Performance Snapshots

Figure A.6.1: Ourknock knees colliding during the jumping phase. A frame-by-frame analysis of our jumper shows this occurring twice during the jump, a likely source of losses during the leap.

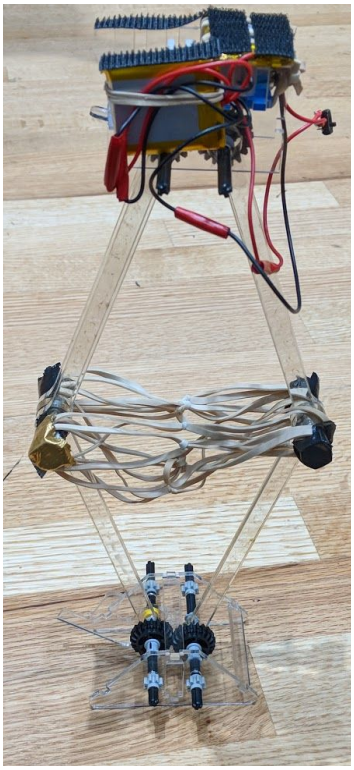

Figure A.6.2: The final version of Ourknock on testing day.